

ENHANCEMENT AND QUENCHING OF PHOTOIONIZATION IN RARE GAS MIXTURES

by

R. Reininger, V. Saile

Hamburger Synchrotronstrahlungslabor HASYLAB at DESY

P. Laporte

Equipe de Spectroscopie C.N.R.S., Saint Etienne

I.T. Steinberger

Racah Institute of Physics, The Hebrew University, Jerusalem

Eigentum der Property of	DESY	Bibliothek library
Zugang: Accessions:	- 5. JULI 1984	
Leihfrist: Loan period:	7	Tage days

DESY behält sich alle Rechte für den Fall der Schutzrechtserteilung und für die wirtschaftliche Verwertung der in diesem Bericht enthaltenen Informationen vor.

DESY reserves all rights for commercial use of information included in this report, especially in case of filing application for or grant of patents.

To be sure that your preprints are promptly included in the
HIGH ENERGY PHYSICS INDEX ,
send them to the following address (if possible by air mail) :

DESY
Bibliothek
Notkestrasse 85
2 Hamburg 52
Germany

Enhancement and quenching of photoionization

in rare gas mixtures

R. Reininger^(a), V. Saile^(a), P. Laporte^(b) and I.T. Steinberger^(c)

(a) Hamburger Synchrotronstrahlungslabor HASYLAB / DESY, Notkestr. 85,
D-2000 Hamburg 52, Germany

(b) Equipe de Spectroscopie C.N.R.S. (LA 171), 158 bis cours Fauriel,
F-42023 Saint Etienne Cedex, France

(c) Racah Institute of Physics, The Hebrew University of Jerusalem,
Jerusalem, Israel

Abstract

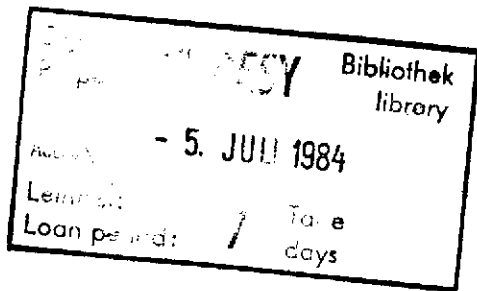
Admixing a sufficient amount of a light rare gas to a heavier one enhances the photoionization current at the absorption lines of the latter provided the exciting photons satisfy $h\nu > E_c$ and quenches it if $h\nu < E_c$. E_c is approximately equal to the ionization potential of the corresponding heteronuclear dimer. Homonuclear and heteronuclear dimer ion formation are both discussed.

Rare gases can be ionized by photons having energies below the first ionization potential of the respective atoms but above the energy difference between the lowest vibronic state of the dimer ion and the ground state of the free atom [1-3]. For low densities, this ionization occurs at atomic absorption lines, but with increasing density the photoresponse extends to higher and higher intervals around the atomic line, coalescing eventually (for densities of the order of 10^{19} cm^{-3} and above) to a single continuum interrupted by broad dips centered roughly at the positions of the atomic lines [3]. The basic interpretation of these results in the framework of the quasi-static broadening theory rests upon the formation of excimers as a result of photon absorption, followed by ionization and dimer ion formation. In such experiments increasing the density may have two effects: a) increasing the number of pairs that can lead to excimer formation; b) increasing the number of atoms that may interfere with dimer ion formation from the excimer.

It is desirable to separate effects "a" and "b"; this is possible, in principle, by studying the photoionization process in a given gas at a low density and noting the subsequent changes caused by the admixture of increasingly larger amounts of another, lighter perturbing gas. One aspect of this work is the study of the influence of a foreign gas on homonuclear excimers.

In a mixture of two rare gases heteronuclear excimers can also be created by incident radiation, their formation probability increasing with increasing density of both constituents. Density-dependent photoionization spectroscopy, as presented in this paper, can give valuable information on the heteronuclear dimers and the corresponding dimer ions as well. Such measurements complement the extensive work by Ng et al [4] and Dehmer et al [5,6] employing photoionization mass spectroscopy of Van der Waals dimers created in a supersonic beam.

For the experiments described below a special cell was fabricated equipped by a pair of very thin ($\approx 80 \text{ nm}$) indium foils stretched on a fine (35μ) copper mesh. These foils served as entrance and exit windows for monochromated synchrotron radiation, making possible to take absorption spectra and also as electrodes for the measurements of the photoionization currents. The windows were isolated from the stainless-steel cell body by ceramic rings; the distance between the windows was $\approx 3 \text{ mm}$. The diameter of the windows was 7 mm , but only a circular area of $\approx 2 \text{ mm}$ diameter was left clear from its substrate to let the light through. Only low vapour-pressure epoxy resin was employed to glue together various parts of the cell.



The spectral transmittance of the empty cell in the region of 90 nm was of the order of 0.1 %; the leak rate through microscopic defects of the foils dp/pdt , p being the total pressure and t the time, was typically about 0.2 hour^{-1} . The photoionization currents were measured by using essentially DC methods, while the transmitted light intensity was measured by photon counting techniques. Because of the very strong absorption of the windows the transmission spectra were rather noisy. They served for wavelength calibration and as indicators of the transmission level of the filled cells but their quality was insufficient for making quantitative comparisons with the photoionization current peaks. In the experiments the recorded width of the absorption and photoionization lines was determined by the spectral resolution (0.03 nm). The results refer to the gas mixtures Xe:Kr, Xe:Ar, Kr:Ar and Kr:Ne, the first gas having a low density ($3.5 \times 10^{16} \text{ cm}^{-3}$) and that of the second lighter gas varying up to about $7 \times 10^{18} \text{ cm}^{-3}$. While recording a spectrum the two densities could vary up to about 20 %, because of the leaky indium windows, but in most cases the cell was continuously replenished by the lighter gas by means of a needle valve. All measurements were performed at room temperature. Typically, a potential difference of 25 volts was applied between the two electrodes, the front electrode being negative.

The photoionization currents measured (I) were divided, for quantitative discussion, by the background of the transmitted light intensity T_0 (ignoring the absorption lines). This normalization was necessary to compensate for the eventual effects of slightly varying positions of the incident synchrotron radiation. Figure 1 shows the photoionization current thus normalized as a function of the wavelength for krypton at a density of $3.5 \times 10^{16} \text{ cm}^{-3}$ (a), the normalized photoionization current for a mixture of $3.5 \times 10^{16} \text{ cm}^{-3}$ Kr and $2.7 \times 10^{18} \text{ cm}^{-3}$ Ar (b) as well as the transmission spectrum of the mixture (c). The identification of the krypton and argon spectral lines is also included [7,8]. The continuous background of the photocurrent spectra is due mostly to photoemission from the front indium electrode; however, the rise of the background current just before the krypton ionization edge (88.56 nm) is probably caused by collisional ionization of excited Kr atoms [9]. For a pure krypton sample photoionization appears at all stronger lines below 95.34 nm (the figure shows only the region below 95.5 nm), i.e. at photon energies roughly above the ionization potential of the Van der Waals molecule Kr_2 (96.367 nm, ref. [10]). In the Kr:Ar mixture ("b" in Fig. 1), however, the photoionization at the 92.27 nm line as well as at all lines at wavelengths above this limit becomes quenched. On the other hand, photo-

ionization lines at shorter wavelengths are considerably stronger than in the spectrum of the pure krypton sample. The same behaviour was found in the other rare gas mixtures investigated as well: at a sufficiently high pressure the perturbing gas quenches the photoionization below a certain photon energy E_c and enhances it above this limit. This is, indeed, the central result of the present work.

Figure 2 shows the ratio $R \equiv (I - I_0)/T_0$, I_0 being the photocurrent background, as a function of the total density ρ for several wavelengths in the Kr:Ar system, the krypton density ρ_{Kn} being kept at the constant value of $3.5 \times 10^{16} \text{ cm}^{-3}$. It is seen that at the longest wavelengths the photoionization is quenched for all $\rho > 0.2 \times 10^{18} \text{ cm}^{-3}$, becoming negligible for $\rho \geq 2.8 \times 10^{18} \text{ cm}^{-3}$. For somewhat shorter wavelengths R goes at first through a pronounced maximum at a low density followed by quenching to a low level. This level increases with decreasing wavelength until the maximum in the curve disappears and the R vs. ρ curve has a positive slope throughout, becoming linear for higher densities.

It is convenient to employ a consistent quantitative definition for the threshold energy E_c for all mixtures: E_c is a photon energy such that for $h\nu \geq E_c$ $R(\rho) > 0.5 R(\rho_0)$ and for $h\nu < E_c$ $R(\rho) \leq 0.5 R(\rho_0)$, provided $\rho \geq 100 \rho_0$. ρ_0 denotes here the density of the pure "solute" gas (Kr in the above case; $\rho_0 = 3.5 \times 10^{16} \text{ cm}^{-3}$). The values of E_c thus defined for the Kr:Ar system and for several other systems appear in Table 1. It is seen that E_c decreases with the atomic weight of both gases for the mixtures investigated.

The simplest qualitative interpretation of the above results is as follows. Denoting the heavier solute atom by Y and the lighter solvent atom by X, the photon energy E_c is approximately equal to the energy difference between the lowest vibronic state of the $A_{1/2}^{2\Sigma^+}$ heteronuclear dimer ion (which dissociates to $X(^1S_0) + Y^+(^2P_{3/2})$ [6]) and the ground states of the atoms X and Y. If $h\nu \geq E_c$, photoexcitation in the rare-gas mixture can result - after some intermediate processes - in the formation of a heteronuclear dimer ion XY^+ and a free electron.

For photon energies $h\nu < E_c$ the above process is energetically impossible; the only way of creating a free electron is by a simultaneous formation of a homonuclear dimer ion Y_2^+ . To deal with the observed quenching, one

has to consider the possible effects of the solvent gas on the processes leading to Y_2^+ and the free electron. Quenching may be caused, in principle, in two different ways: a) If the homonuclear dimer ions Y_2^+ are formed predominantly as a result of collisional ionization [2,11] $Y^* + Y + Y_2^+ + e^-$, the presence of many X atoms may prevent the process simply because collisions of Y^* with an X atom would have a much higher probability. b) If the formation of the homonuclear dimer ion has to be described on the basis of quasi-static concepts [3], namely $(Y + Y) + h\nu + Y_2^*$, followed by $Y_2^* + Y_2^+ + e^-$, quenching could be caused by dissociation of the Y_2^* excimers upon collision with an X atom. However, it seems that for the prevailing low densities of the Y atoms the "quasi-static" formation of Y_2^+ should be only of minor importance. Thus the collision of a X atoms with an excited Y^* atom should be the main cause for quenching. Assuming this mechanism, one may give a tentative explanation for the shape of the quenching curves of Figure 2. One has to take into account the further fact that the energy of an excimer XY^* is usually higher than of a free electron plus a YY^+ homonuclear dimer ion, therefore, transfer of excitation from one system to the other should be possible, probably by appropriate collisions. Thus at relatively low solvent densities there may be an increase of the photoionization current when compared with the pure solute. At higher densities, however, the quenching by process "a" (as a result of many X atoms surrounding each Y atom) would be overwhelming, as observed.

A comparison of the E_c -values formed in this work with the adiabatic ionization potentials I_G of the corresponding heteronuclear Van der Waals molecules, as determined by photoionization mass spectroscopy on molecular beams [4-6] also appears in Table I. It is seen that there is a close correspondence between the two sets of values, though the differences are well beyond the experimental error. These differences stem from the somewhat arbitrary definition of E_c as well as from the fact that with the method described we have no information about regions between the absorption lines. Ultimately, however, the differences between E_c and I_G also depend on the detailed behaviour of the potential curves of the heteronuclear excimers.

The authors wish to express their thanks to Mr. H. Zeiger for the extremely careful preparation of the indium windows.

References

- 1 J.A.R. Samson and R.B. Cairns, J. Opt. Soc. Am 56 (1966) 1140.
- 2 R.E. Huffman and D.H. Katayama, J. Chem. Phys. 45 (1966) 138.
- 3 P. Laporte, V. Saile, R. Reininger, U. Asaf and I.T. Steinberger, Phys. Rev. A28 (1983) 3613.
- 4 C.Y. Ng, P.W. Tiedemann, B.H. Mahan and Y.T. Lee, J. Chem. Phys. 66 (1977) 5737.
- 5 P.M. Dehmer and S.T. Pratt, J. Chem. Phys. 77 (1982) 4804.
- 6 S.T. Pratt and P.M. Dehmer, J. Chem. Phys. 76 (1982) 3433.
- 7 K. Yoshino and Y. Tanaka, J. Opt. Soc. Am. 69 (1979) 159.
- 8 K. Yoshino, J. Opt. Soc. Am. 60 (1970) 1220.
- 9 K. Radler and J. Berkowitz, J. Chem. Phys. 70 (1979) 221.
- 10 S.T. Pratt and P.M. Dehmer, Chem. Phys. Lett. 87 (1982) 533.
- 11 J.A. Hornbeck and J.P. Molnar, Phys. Rev. 84 (1951) 621.

Table 1

Absorption lines corresponding to E_c (see text) for the different rare-gas mixtures measured. The adiabatic ionization potentials I_G for the heteronuclear dimer are also listed for comparison.

	Designation	E_c (eV)	I_G (eV)	
Xe Kr	$9d[1/2]_1^o$	11.801	$11.757^{(a)}$	$11.763^{(b)}$
Xe Ar	$13d[3/2]_1^o$	12.013	$11.985^{(a)}$	$11.968^{(b)}$
Kr Ar	$7d[3/2]_1^o$	13.600	$13.425^{(a)}$	$13.484^{(b)}$
Kr Ne	$13d[3/2]_1^o$	13.903	$13.950^{(c)}$	

(a) Ref. [4]

(b) Ref. [5]

(c) Ref. [6]

Figure captions

Figure 1 Normalized photocurrent (see text) for: a - $3.5 \times 10^{16} \text{ cm}^{-3}$ krypton and b - a mixture of $3.5 \times 10^{16} \text{ cm}^{-3}$ krypton and $2.7 \times 10^{18} \text{ cm}^{-3}$ argon. c - transmission spectrum of the mixture.

Figure 2 Photoresponse as a function of the total density for several krypton atomic lines. The krypton density as in fig. 1. ∇ - 94.65, o - 92.27, x - 91.17, Δ - 89.67 and \square - 89.08 nm.

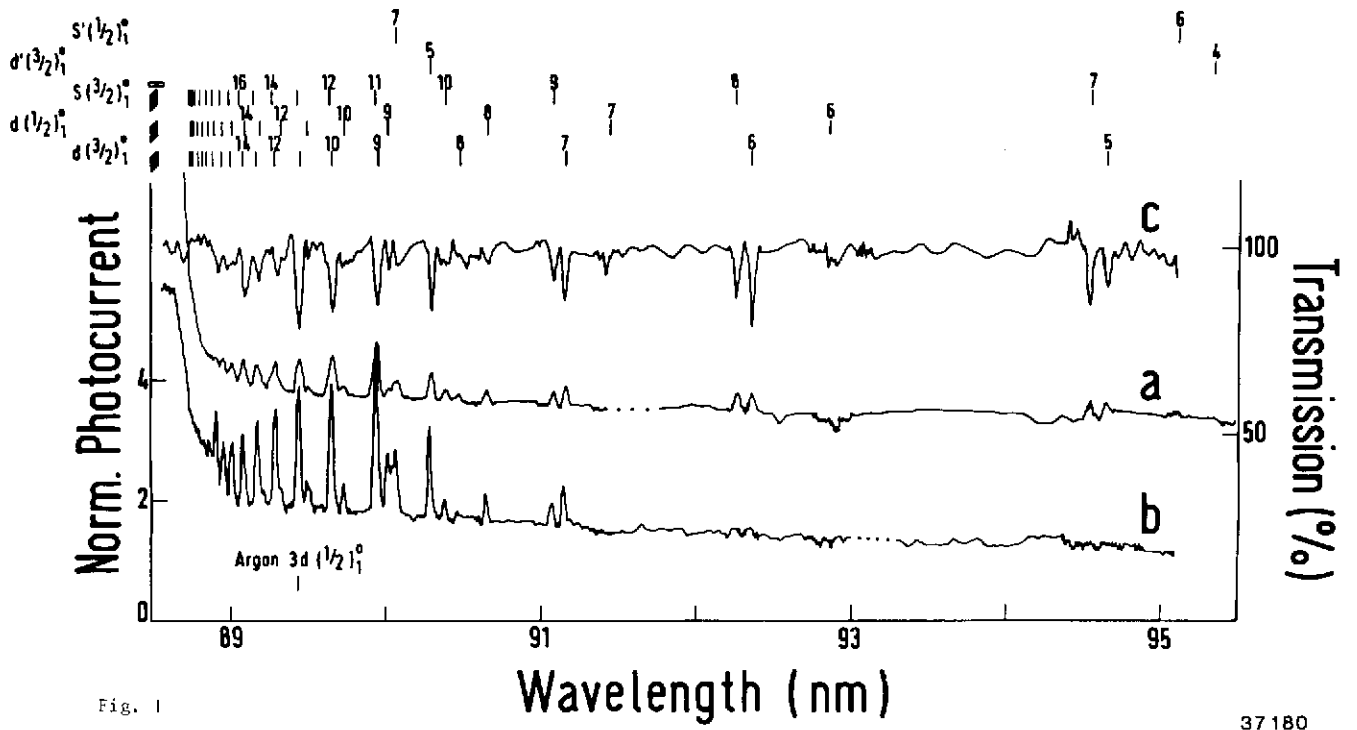


Fig. 1

37 180

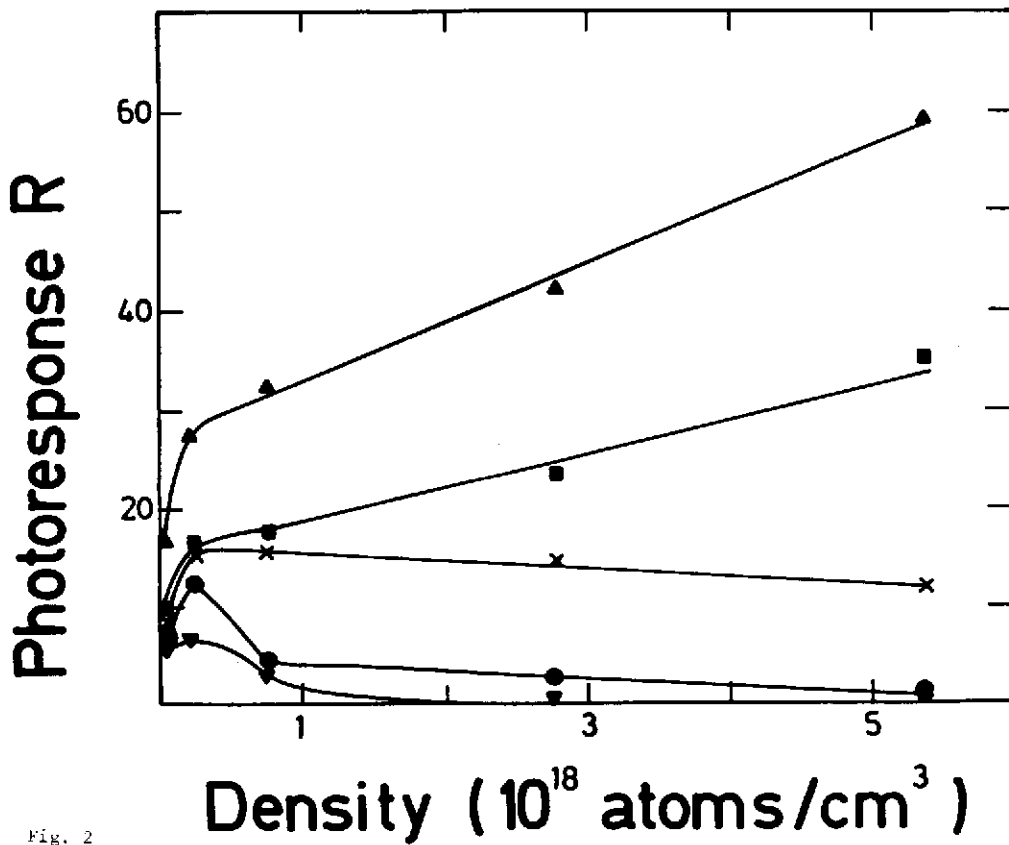


Fig. 2

37 181

